FR9300464
CEA-CONF--11129

EXPERIMENTS ON VIBRO-IMPACT DYNAMICS OF LOOSELY SUPPORTED TUBES UNDER HARMONIC EXCITATION

F. AXISA and P. IZQUIERDO

Commissariat à l'Energie Atomique - Centre d'Etudes de Saclay

ABSTRACT

Computational methods have been recently developed by the authors and others to predict the working life or the acceptable vibration limit of tubular structures experiencing fretting-wear caused by impact-sliding interaction with loose supports or adjacent structures. This problem is of practical interest in various nuclear and other industrial components. This paper reports an experimental work intended to validate the numerical techniques used to compute the tube non-linear vibration in presence of impact-sliding interaction. Attention is especially focused on the local and time averaged dynamical parameters governing the rate of fretting-wear. The experiments were carried out on a straight tube excited harmonically by a pair of electromagnetic shakers. The tube motion was limited by a loose support situated at about midspan. On the other hand, numerical simulations of the tests were also performed. Comparison between test and computational data resulted in rather satisfactory agreement, based on the averaged impact forces and the wear work rate. Results are also discussed in terms of detailed time histories of tube displacement and impact forces.

1 INTRODUCTION

It is now generally recognized that the service life of various tubular components in nuclear power reactors can be significantly

shortened because of excessive wear caused by the sliding-impact interaction with neighbouring structures and/or loose supports. This can be typically the case for the steam generator tubes, the in-core instrumentation, the fuel and the control rods, which are permanently excited by the coolant flow. Prediction of such a risk requires the use of numerical tools to compute the flow-induced vibrations of the components. As pointed out in several recent studies, see for instance Axisa, et al.(1986); Moon, (1987); de Langre et al.(1990,1991); such highly non-linear systems can have a large variety of dynamical behaviours, which can be sensitive even to very small changes in the initial conditions and system parameters, including the numerical errors involved in the computational process. However, from a practical point of view, interest can be basically focused on the behaviour of a few averaged dynamical quantities, the ones most relevant for assessing the wear. Hopefully, those quantities are significantly less sensitive than the detailed time histories of the dynamical response.

Computational methods have been developed by several authors, in particular Rogers and Pick (1977); Frick et al. (1984); Axisa et al.(1986); Rao et al.(1987); Antunes et al.(1988); Fricker, (1988); Mahutov et al. (1989) to deal with some aspects or to cope with the overall problem of flow-induced vibration and wear of tubular structures.

Laboratory experiments are also necessary to verify the validity of the numerical models used in the non-linear calculations. Indeed, to make the problem practically tractable for design analyses, many simplifying assumptions are made to model the vibrating structure, the tube-support dynamic interaction, and the flow-induced excitation mechanisms. On the other hand, it is also of major importance to investigate how closely the measured values of averaged dynamical quantities such as the wear work rate can be compared with the computed ones. This is by no means a trivial experimental problem, in particular because impacts occur as local and short lived impulses and because tube sliding distances cannot be measured at the very location where impacts actually take place.

The present work is more specifically focused on the last aspect of the problem. It describes experiments which were carried out on a straight tube harmonically excited either in one or in two lateral directions, by electromagnetic shakers. Tube vibration was restricted at midspan by a stiff support surrounding it. Pure

impact and impact-sliding interaction were successively investigated. Results are discussed together with numerical simulations, in terms of detailed time histories of the response signals and in terms of averaged dynamical quantities, namely the rms tube displacement, the time averaged impact forces and the averaged wear work rate.

2 EXPERIMENTAL SETUP

Test Rig

A general lay-out of the test rig is shown in Fig.1. The tube is representative of a PWR fuel rod, with overall length L = 1.25 m, diameter D = 9.5 mm and mass per unit tube length M = 0.7 kg/m. It is firmly maintained at both ends by stiff springs, and at about midspan it passes through the cell shown in Fig.2. Though contacts can actually occur only at the flat bumped parts of the cell, the latter acts essentially as a square hole loose support with total gap of about 0.2 mm. It is embedded into a measuring device shown in Figs. 3 and 6, which includes four prestressed piezoelectric Kistler force transducers 9301 A, each of which is associated to a distinct wall of the support cell, and two pairs of displacement transducers Kaman 2310 2S. One pair is located above and the other below, the cell, about 5 cm from its median plane where intermittent contacts with the vibrating tube occur. The whole measuring device is rigidly fixed to a pair of micrometer MICROCONTROL tables whose purpose is to adjust the gaps at the desired values, including negative ones in order to pre-stress the vibrating tube by a static side load. All the instrumentation is set along the X,Y directions, perpendicular to the walls of the support cell. Fig.4 shows the pair of electromagnetic shakers used to excite the tube. They are mounted along the X,Y directions, and sufficiently close to the bottom support so as to reduce the dynamical interaction between the tube and the exciting device. Amplitude of the harmonic excitation was varied from a few tenths up to 10 N. Depending on the relative phasing between the shakers, the tube can be driven either according to unidirectional or to orbital transverse motions. The driving force signals are measured by using two piezoelectric impedance heads B&K 8001, mounted on the head of the shakers. Fig.5 provides the reader with the exact geometry of the tube mounting used for the orbital tests. It is noticed that the end supports are modelled as a set

of three lateral springs which actually correspond to three distinct permanent contacts between the tube and the support. Value of the stiffness coefficients was adjusted by performing modal measurements, see section 3.4.

3 EXPERIMENTAL AND NUMERICAL PROCEDURES

Experimental Data Processing

The signals produced by the instrumentation just described are tape recorded and then numerized at a sampling frequency f_e of about 50 kHz. Practical relevance of such a value was checked by performing preliminary tests at higher f_e, up to 100 kHz. The data were processed in a HP 9000 computer by using specific software, to obtain the time averaged quantities, namely the impact forces: $\langle F_c \rangle$; the wear work rate: $\langle \dot{W} \rangle$; and the rms values σ_x, σ_y of the displacements. Clearly, the first two parameters are the least easy to obtain as they are very sensitive to the presence of background noise and offset in the measured signals. A rather tedious effort was necessary to conveniently process the signal and to check the results, which convinced us that a relative accuracy better than about 50% can reasonably be expected in the present study, where the signals are averaged typically over 600 excitation cycles. On the other hand, the analog signals were also systematically transferred to a GOULD recording system for graphical display of the time histories at different time scales and sampling rates. Lissajous plots of the transverse tube displacement were also produced. Such graphical information is quite useful to get a qualitative picture of the tube motion near the loose support.

Calibration of the Impact Force Transducer Assembly

The force transducer assembly was tested according to an experimental procedure described in Axisa, et al.(1989), which is similar to that used by Fisher, et al.(1988), except that in our tests the steel ball impacting the sensor is mounted as a pendulum, instead of as a free falling projectile. Furthermore, the calibration is not relying upon the peak force but on its time averaged value. Indeed, the last quantity provides the momentum change of the ball due to the impact. Then, by comparing it with the theoretical value of a pure elastic impact, it is possible to

obtain a reasonable order of magnitude for dissipation. The latter is entered in the numerical simulations as an equivalent impact restitution coefficient: r. On the other hand, in this kind of tests, the measurement of the impact duration has to be interpreted in terms of the Hertzian contact theory , as pointed out in Fisher and Ingham (1988) and Axisa, et al.(1989). Nevertheless, it can still be used to check the validity of the equivalent impact stiffness which is adopted in the numerical simulations.

Fig.6 sketches the testing procedure used in the present experiment. Because of obvious geometrical reasons, the ball cannot hit the support cell directly. Thus, a steel rod is used to transfer the impact of the ball to the support cell. Such tests were performed first by removing the cell to check the whole assembly, including the micrometer tables, against undesirable impact transmission from one force transducer to the others and against an excessive flexibility of the measuring assembly mounted on the rig. Fig.6 also shows a typical time history of such an impact as measured by the impacted transducer:(A), and the two adjacent ones: (B,C). It can be verified that the impact signature is satisfactory. In particular, the vibration detected on the (B,C) channels is small, with maximum amplitude being 1% of that of channel (A). The signal recorded on channel (D) facing (A), is not shown here because its amplitude was quite negligible. Furthermore, the impact duration recorded on channel (A) is about $1.6\ 10^{-4}$s, which leads to an equivalent stiffness of $1.1\ 10^{7}$N/m. This value is larger by one order of magnitude than the expected impact stiffness associated with the support cell and the tube ovalization. The coefficient of restitution is 0.95. Similar tests performed with the support cell inserted in the device led to an equivalent stiffness of 10^{6}N/m; by chance this value is nearly the same as the ovalization stiffness of the tube. Finally, r was found to be significantly less than in the former case : 0.8 instead of 0.95.

Numerical Simulations

The results quoted above lead to an equivalent impact stiffness K_c of about 6×10^{5}N/m, which corresponds essentially to the generalized stiffness of the 6th flexural mode, see Table 1. Hence, the dynamical non-linear model can be safely restricted to 6×2 D.O.F. taking into account the two transverse directions X,Y.

Accordingly, the shortest period is 0.44 ms. A sufficient accuracy of the Fu-Devolegeare explicit algorithm, see Axisa et al. (1986), is reached by adopting a time step $\delta t = 8.68\ 10^{-5}$s, when dry friction is neglected. When it is modeled according to the method described by Antunes et al.(1988), it is preferable to divide the above δt by 3. The time histories of the relevant signals were computed during about 120 cycles of the driving force, requiring thus 370000 time steps when dry friction is included in the model. It was found that the tube non-linear response becomes essentially steady after about 20 cyc- les. Hence, the time averaging was limited to the last 100 cycles of the computed signals to obtain the desired mean quantities. However, it has to be emphasized that the non-linear dynamical regime of the tube can still vary significantly over time scales larger than . cycles, in agreement with de Langre, et al.(1991). Here, this was observed to be the case, especially as the wear work rate is concerned, due to variations in the sliding distances. Based on a few numerical simulations made over more than 100 cycles, statistical errors larger than 30% are not expected, as wear work rate is concerned, which is the most sensitive of the parameters of interest, when the signals are integrated over 100 cycles.

Modal Analysis

Before starting the non-linear tests, the first six flexural modes of the tube installed in the rig were measured in the X,Y directions in order to adjust the numerical model in relation to the stiffness of the firm end supports and the modal damping. The results are given in Table 1. From this study the following points are worth noting,

(1) the relative errors on natural frequencies between tests and calculations are less than 4% for the whole modal set, and less than 0.4% as far as the first mode is concerned.

(2) The end supports are nearly clamping the tube. However, they have some flexibility which slightly differs in the X and Y directions. The computational model used $K_{1X} = 1.2\ 10^6$ N/m and $K_{1y} = K_{2X} = K_{2Y} = 6\ 10^5$ N/m. These values are of the same order of magnitude as the impact stiffness. This is not surprising because the design of the end supports is similar to that of the loose cell.

(3) Damping depends on the mode considered and it is expected that most of dissipation takes place at the end supports. Repetitive

tests resulted in a rather large scatter in the measured damping of about 20%. In consequence, it was decided to carry out most of the non-linear tests at frequencies sufficiently far from the resonance frequencies so as to minimize the effect of such uncontrollable variations in damping. Furthermore, numerical simulations made us confident that the importance of damping is mainly restricted to low excitation levels, which induce small impacts. Indeed, the resonant behaviour of the tube is rapidly fading out as soon as impacts occur. This was also confirmed by experiment.
(4) Harmonic excitation tests made at f= 11.5 Hz without impacting on the loose support provided relative discrepancies between the computation and measurement of the displacement near the loose support of about 20% . Obviously, such an error has a direct incidence on the final non-linear results. No correction was made for this defect, which was accepted as a factor of experimental inaccuracy.

4 NON-LINEAR TESTS

Unidirectional Excitation Tests

The tube was almost centered within the loose cell; total gap of the latter was 0.2 mm. It was excited at 13.16 Hz, in the X direction. Point of excitation was 7 cm above the lower support. Fig.7 shows typical computed and experimental time histories of the tube response. Case (a) refers to a rather low excitation level producing a periodic motion at the driving frequency with a single impact at each half-cycle. Experiment and computation produce essentially the same results, except for some discrepancies concerning the relative level of the impact signals occuring on both sides of the tube (channels A and D). This can be caused by small experimental errors in the tube centering. In case (b), amplitude of the excitation is ten times higher than in case (a). The computed response is still periodic and the impacts display three distincts peaks, caused by tube rebounds at the support. The experimental response is rather similar to the computed one, except for noticeable differences in the detailed time histories of the impacts which are more violent on channel A than on channel D, and which are no longer periodic, though they are still occuring at each excitation cycle. Case (c) refers to a sligthly higher excitation amplitude than case (b). It can be noticed that the relative agreement between calculated and measured time

histories is significantly better than in case (b). Despite such differences, impact duration is found to be satisfactorily reproduced by computation: 1.7 ms instead of 1.6 ms in case (a), 8 ms on channel A in case (b) instead of 8.5 ms and 8 ms instead of 9.5 ms in case (c). This is in good support of the choice of impact stiffness and modal basis made in the simulations. The examples discussed just above are representative of the non-linear behaviour of the tube in similar tests we made during this study and others, Axisa et al.(1989).

Referring now to the time averaged quantities, it is found that experiment and computation agree reasonably well with each other. Indeed, relative discrepancies were less than 20% on σ_x and less than 30% on $\langle F_c \rangle = \langle F_c \rangle_A + \langle F_c \rangle_D$, summation on the two impacted channels allowing to smooth out the miscentering effects of each individual channel. In agreement with former published results, Axisa, et al.(1984); Ko (1985); Axisa et al.(1989), $\langle F_c \rangle$ is proportional to the excitation level and fairly insensitive to the tube centering and to the tube/support gap, as soon as the impacts become sufficiently large, see Fig. 8.

Orbital Motions

Tube centered with respect to the loose support

Series of tests were performed at a driving frequency of 11.25 Hz and at distinct excitation amplitudes. The total gaps at the loose cell were 0.15 and 0.16 mm in the X and Y directions, respectively. Fig.9 displays a representative set of measured time histories. At the lowest excitation level, the motion is still periodic and the impacts occur as single isolated peaks. This test is rather peculiar as the period of impacts is observed to be twice the excitation period. It seems that this kind of motion holds only in a fairly narrow range of parameters because simulation and tests repeated at nearly the same conditions produced a periodic motion at the driving frequency instead of the first bifurcated dynamical regime mentionned here. According to experiment and calculation, the impacts become multipeaked and the motion looses its periodicity when the excitation level is increased. The averaged quantities are reported in Table 2. From these data the following major points arise:

(1) the agreement in the rms displacements is to within 20%, the

test data being larger than the computed ones,

(2) the total contact times over a driving cycle agree to within 15%, except at the lowest excitation level where discrepancies as large as 50% can be noted,

(3) the averaged impact forces agree to within 40%, based on the summation of the four channels, the test data being smaller than the computed ones. Test series were repeated in an attempt to investigate the experimental scattering, which was found to be generally less than 10%, except at the lowest excitation level, where it was significantly higher (about 50%).

(4) Wear-work-rates agree to within 40%, and often to within 15%, also based on the summation of the four channels. Test data are again smaller than computed ones.
Furthermore, according to experiment and calculation, both total impact force and wear-work rate are found to increase almost linearly with excitation level. Finally, a reasonable fit can alsobe obtained by using the simplified formulation given in Axisa, et al.(1986).

$$\dot{\langle W \rangle} = 4\sqrt{2}\ f\ \sigma\ \langle F_c \rangle$$

where f is the basic cycle of the tube displacement, $\sigma = \sigma_x = \sigma_y$.
Experimental data were used to derive the values given in Table 2.
Series of tests were also performed in which the frequency of the excitation was varied and its amplitude was kept constant: $F_x = F_y = 5$ N. The tube orbits were found to vary significantly with frequency, as illustrated in Fig.10 which also puts in evidence the rather good agreement between the major features of the computed and the measured Lissajous plots. The rms displacement at the lower position of the Kaman sensors was found to be essentially insensitive to the excitation frequency, and values of about 70 and 85 μm were found by experiment and computation, respectively. Averaged impact forces increase almost linearily with frequency; this is caused mainly by an increase in the number of impacts and not by higher peak values of the force signals. Wear work rate increases with frequency according to parabolic law, as expected from eq. (1). The relative agreement between test data and computed values in this test series was better than 20%., see Fig. 11.

Tube deflected by a lateral static load

These tests were performed by displacing the micrometer table in the X direction to deflect the tube statically. The magnitude of the preload was obtained by measuring the transient signal delivered by the contact force transducer, when the tube was suddenly removed from contact. Another method was to measure the oscillatory contact reaction in relation to the excitation level. Indeed, as soon as the preload becomes less than the amplitude of the support reaction, contacts become intermittent and the presence of impacts is clearly detectable on the force signal. Preloads were varied from 0.05 up to 1.N. Fig.12 refers to a preload of 0.1 N. For $F_x = F_y = 2$ N, the tube experiences pure sliding on the loaded cell wall and impacts on the adjacents ones. The time histories of the tube displacement in the sliding direction displayed in Fig.12-a differ significantly from each other depending on the sensor location. It can also be verified that the computed time histories are in close agreement with the experimental ones. The measured contact force was found to be roughly sinusoïdal, with a peak to peak amplitude of about 0.16N instead of 0.2N according to computation; displacement in the preload direction was less than 10 µm and the wear work rate was 0.3 mW, instead of 0.4 mW. For $F_x = F_y = 4$ N, the tube is impacting the preloaded cell and the two adjacents ones. The computed and experimental time histories of the displacement in the X and Y directions are again in satisfactory agreement, except that the computed signal in the preload direction is less regular than the experimental one.

Table 3 provides information concerning the averaged parameters. Large discrepancies between test and computed data for σ_x and $\langle W \rangle$ are obvious for the lowest excitation levels. The same behaviour was noticed in the tests made with larger preloads. This is interpreted to be the consequence of some uncertainties on the preload and the friction coefficient. Indeed the stick-slip transition is found to be rather abrupt, according to simulations and experiments.

Tests carried out at fixed excitation and distinct preloads are evidencing that the wear work rate is steadily increasing with the preload as far as its value remains sufficiently low to prevent any take-off from the loaded support, then it becomes poorly dependent on the preload up to the values at which sliding is also prevented. Table 4 illustrates the first two steps of such a behaviour. For the excitation considered: $F_x = F_y = 4$ N, the range

of preloads where sliding is prevented was not explored. According to Antunes, et al.(1988) it leads to an abrupt decrease in wear work rate. Finally, it was verified that eq.(1) fits the data even better than in the absence of preloads. This could be expected a priori, because the preload is increasing significantly the relative importance of sliding over impacting tube/support interaction.

5 CONCLUDING REMARKS

An experimental study to investigate the vibro-impact response of a loosely supported tube to harmonic excitations has been presented. A rather large number of tests have been carried out by changing the excitation parameters and the support conditions, in order to explore various dynamical conditions which can be met in practice. The few results discussed here were selected among a much larger data set which produced similar results, based on which the following major points can be emphasized concerning the validation of the numerical methods,

(1) As expected, significant differences are often present between the computed and measured detailed time histories of the response signals, and this is particularily true for the impact forces. Nevertheless, striking similarities are also clearly apparent, which are worth pointing out.

(2) Concerning local quantities such as the averaged impact forces and the wear work rate a reasonably good agreement was achieved between computation and experiment. This is further stressed out in the regression plots given in Figs.13 and 14, which incorparate the various test conditions described above. It can be noted that the regression line is barely different from the ideal one. More points could be added to these plots by using data available at preloads larger than 0.2N. The fit would be even better but nothing much new would be learned, because in most of such additional tests $\langle F_c \rangle$ is dominated by the oscillatory component at the preloaded support and $\langle W \rangle$ is dominated by the pure sliding component. In such cases, experiment and computation become much easier than in configurations dominated by impact-sliding tube/ support interaction.

(3) The present study is pointing out several difficulties present

in the assessment of the accuracy of the wear work rate which can be expected from numerical simulations. Indeed, the relative error between experiment and computation is found to be governed by experimental errors which are hard to control, and by the nature of the tube motion which is often found to be intrinsically irregular (or chaotic) in the presence of impact-sliding interaction. In consequence, the goodness of the fit between experiment and simulation can vary to a large extent depending on the dynamic regime tested.

Based on the present study, in which a few data were removed because of obvious difficulties in reproducing the actual impact and stick-slip conditions when the excitation level is too small, it can be stated that test and simulation data agreed together within an error margin better than ± 25% concerning the averaged impact forces, and better than ± 50% concerning the wear work rate. Clearly, one has to recognize that such figures remain closely related to the specific study described here. However, we believe that they strongly support the basic validity of the numerical models adopted in Axisa, et al.(1986); Antunes, et al.(1988), to compute the non-linear tube vibrations in presence of impact-sliding interaction.

AKNOWLEDGEMENTS

This work was carried out as part of a joint Research and Developpement Program between CEA and FRAMATOME: F.A 5132. The numerical simulations were performed with the very valuable assistance of T. Coq from CISI Engineering.

TABLE 1: Modal quantities of the the tube, free at midspan

Mode	Computation		Experiment	
index	Freq.(Hz)	Mass (Kg)	Freq.(Hz)	Damp.(%)
1 X	12.53	0.345	12.51	0.59
1 Y	13.16	0.334	13.21	0.52
2 X	33.52	0.376	33.59	1.44
2 Y	35.15	0.368	36.08	1.32
3 X	65.21	0.368	68.68	1.57
3 Y	68.20	0.364	70.86	1.39
4 X	108.0	0.357	109.8	2.34
4 Y	112.7	0.359	116.9	1.88
5 X	162.1	0.338	164.5	1.49
5 Y	168.9	0.343	172.9	2.40
6 X	227.4	0.322	222.4	1.18
6 Y	236.8	0.329	232.9	2.50

TABLE 2: Averaged dynamical quantities
(tube in the centered configuration, f_e = 11.24 Hz)

F_x (N)	1.	2.	2.	3.	3.	4.	5.	6.
F_y (N)	0.5	1.	2.	2.	3.	4.	5.	6.
T_c(%) Comp.	11.	17.	21.	24.	23.	41.	51.	*
T_c(%) Meas.	5.	19.	24.	24.	26.	41.	60.	*
σ_x(µm) Comp.	54.	59.	61.	63.	60.	65.	68.	*
σ_x(µm) Meas.	66.	70.	66.	70.	70.	66.	80.	85.
σ_y(µm) Comp.	54.	52.	60.	58.	68.	68.	70.	
σ_y(µm) Meas.	62.	66.	66.	66.	75.	80.	88.	90.
F_c(mN) Comp.	7.5	44.	75.	97.	130.	190.	250.	*
F_c(mN) Meas.	3.5	28.	48.	69.	85.	140.	180.	230.
$\dot{W}$ (mW) Comp.	4×10^{-3}	0.16	0.38	0.46	0.56	1.1	1.6	*
$\dot{W}$ (mW) Eq.(1)	3×10^{-2}	0.13	0.22	0.35	0.48	0.75	1.0	1.2
$\dot{W}$ (mW) Meas.	0.015	0.15	0.28	0.33	0.51	0.82	1.1	1.4

F_x , F_y : amplitude of the exciting forces in the X,Y directions

T_c : total tube/support contact time per excitation cycle

F_c : total time averaged impact force, summed on the 4 cell walls

$\dot{W}$: total wear work rate, summed on the 4 cell walls

TABLE 3: Averaged dynamical quantities
(tube in the preloaded configuration, f_e = 11.24 Hz)

Preload : 0.1 N

F_x (N)	1.	2.	3.	4.	5.
F_y (N)	1.	2.	3.	4.	5.
σ_x(µm) Comp.	157.	165.	180.	190.	210.
σ_x(µm) Meas.	190.	180.	190	200.	200.
σ_y(µm) Comp.	4.	9.	34.	90.	150.
σ_y(µm) Meas.	6.	10.	20.	140.	200.
F_c(mN) Comp.	110.	150.	190.	250.	310.
F_c(mN) Meas.	90.	120.	190.	200.	250.
$\dot{W}$ (mW) Meas.	0.13	0.29	0.35	0.61	1.13
$\dot{W}$ (mW) Comp.	0.38	0.39	0.43	0.55	0.86

Preload : 0.6 N

F_x (N)	3.	4.	5.	6.	7.	8.
F_y (N)	3.	4.	5.	6.	7.	8.
$\dot{W}$(mW) Meas.	2.5	3.	3.3	3.7	3.9	3.9
$\dot{W}$ (mW) Comp.	0.27	0.5	2.3	2.6	2.8	3.1

REFERENCES

ANTUNES,J., AXISA,F., BEAUFILS, B. and GUILBAUD, D.,1988,"Coulomb friction modelling in numerical simulations of vibration and wear work rate of multispan tube bundles ASME winter annual meeting, Symposium on Flow-Induced Vibration in Heat-Transfer Equipment November 27-December 2, 1988, Vol.5 157-176; also in Journal of Fluids and Structures,Vol.4 287- 304, 1990

AXISA,F., DESSEAUX,A., and GIBERT R.J.,1984,"Experimental study of the tube/support impact forces in multi-span PWR steam generator tubes",ASME Winter Annual Meeting, New Orleans, USA, December9-14, 1984,PVP Vol.3 139-144

AXISA,F., ANTUNES,J. and VILLARD,B.,1986,"Overview of numerical methods for predicting flow-induced vibration and wear of heat-exchanger tubes",Proceedings of ASME Pressure and Piping Conference, Chicago, USA, July 20-24 1986 PVP-vol. 104, 147-159; also in Journal of Pressure Vessel Technology Vol. 110, 6-14, 1988

AXISA,F., PAUROBALLY,A., and REMOND,A.,1989,"Predictive analyses of flow-induced vibration and fretting wear in steam generator tubes", International Symposium on Pressure Vessel Technology and Nuclear Codes and Standards, Seoul, Korea, April 19-21 1989 / 2 57-75

FISHER,N.J. and INGHAM,B.,1988,"Measurements of tube-to-support dynamics forces in fretting-wear rigs", ASME Winter Annual Meeting Chicago 1988, Flow-Induced Vibrations in Heat-Transfer Equipments, Vol.5 137-156

FRICK,T., SOBEK,T. and REAVIS,R.,1984," Overview on the development and implementation of Methodologies to compute vibration and wear of steam generator tubes", Symposium on Flow-Induced Vibrations, ASME Winter Annual Meeting, New Orleans, USA, December 9-14, 1984, 149-162

FRICKER,A.,1988, "Numerical analysis of the fluidelastic vibration of a steam generator tube with loose supports", International Symposium on Flow-Induced Vibration and Noise, ASME Winter Annual Meeting, Chicago,USA, November 27-December 2, 1988.

KO,P.L,1985," The significance of shear and normal force components on tube wear due to fretting and periodic impacting. Institute of Mech. Eng. Tribology Group Seminar on Fretting Wear, Nottingham U.K., 1985 April 2-3; AECL Report 8845

de LANGRE,E., DOVEIL,F., PORCHER,G. and AXISA,F.,1990,"Chaotic and Periodic motion of a nonlinear oscillator in relation with flow-induced vibrations of loosely supported tubes" ASME Pressure

Vessel Technology Conference, Nashville, USA, June 17-21, 1990, PVP Vol. 189, 119-126

de LANGRE,E., BEAUFILS,B. and ANTUNES,J.,1991,"The numerical prediction of vibrations in tube bundles induced by cross-flow turbulence" Proceedings of I.Mech E., Flow-Induced Vibrations International Conference, Brighton U.K., 20-22 May 1991; paper C416/085 253-262

MAHUTOV,N, FESENKO,T. and KAPLUNOV,S.,1989,"Dynamics of systems in a liquid flow and structure durability" International Conference on Engineering Aero-Hydroelasticity, Prague, Czechoslovakia, December 5-8, 1989 148-156

MOON,F.C.,1987, "Chaotic Vibration, an introduction for applied scientists and engineers" John Wiley & Sons.

RAO, M., GUPTA, G., EISINGER, F., HIBBITT, H. and STEININGER, D.,1987,"Computer modelling of vibration and wear of multispan tubes with clearances at supports" International Conference on Flow-Induced Vibrations, Bowness-on-Winderere,U.K., May 12-14, 1987

ROGERS,R.J. and PICK,R.J. 1977,"Factors associated with support forces due to heat exchanger tube vibration contact". Nucl. Eng. Design.44 247

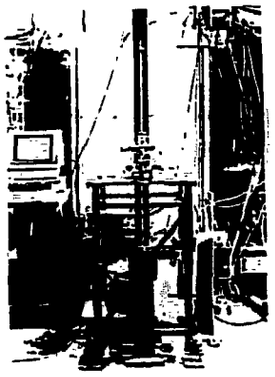

Fig. 1 - The test rig

Fig. 2 - The loose support cell located at tube midspan

Fig. 4 - X, Y exciting shakers

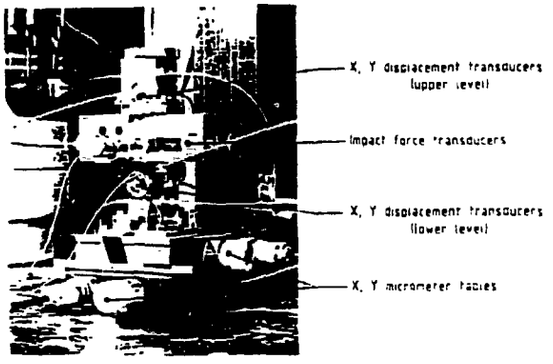

Fig. 3 - The measuring block

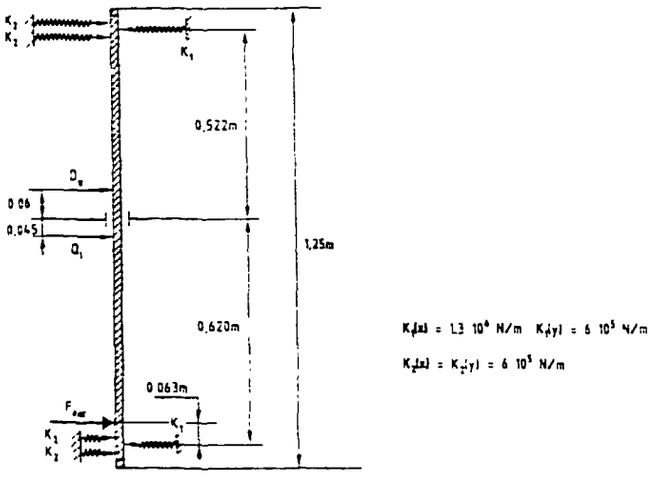

$K_1(x) = 1.3\ 10^6$ N/m $K_1(y) = 6\ 10^5$ N/m

$K_2(x) = K_2(y) = 6\ 10^5$ N/m

Fig. 5 - Geometry of the vibrating system

The spring system K_1, K_2 is modelizing the actual permanent contact conditions at the end supports. The K_2 springs are located at 1.64 and 1.9cm from K_1

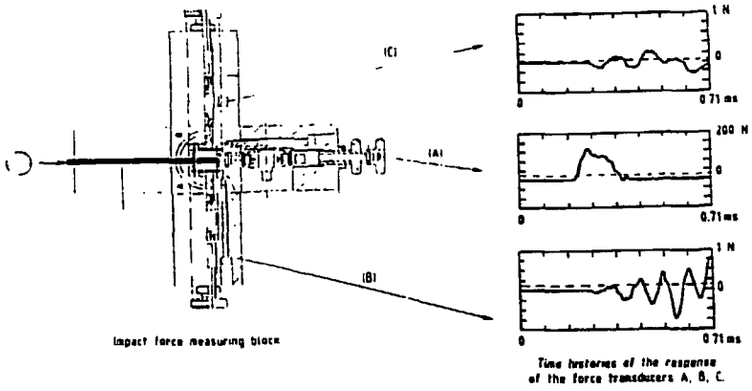

Fig 6 - Test procedure to check the impact measuring device with the loose support set-up

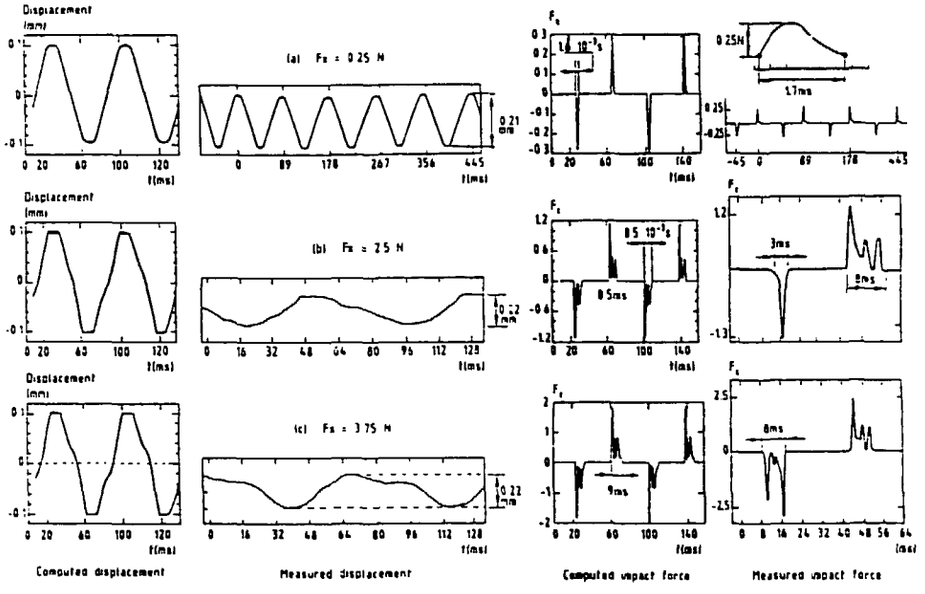

Fig 7 - On directional excitation tests comparison between measured and computed time histories of displacement X(mm) and impact forces (N) time is in ms

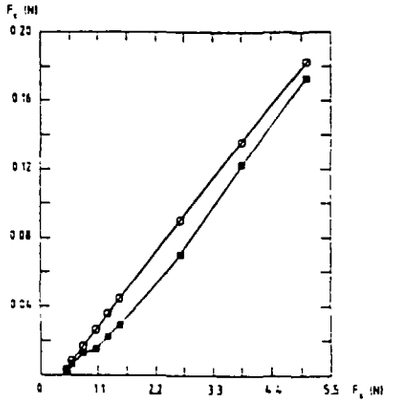

Fig 8 - Time averaged impact forces as summed on the two opposite cell walls

○ Computation
■ Experiment

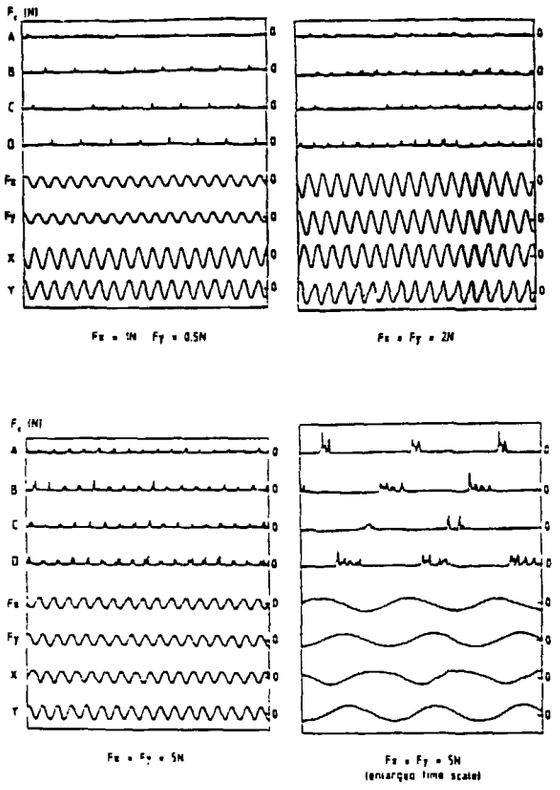

Fig 9 - Time histories of the tube response for centered orbital motions

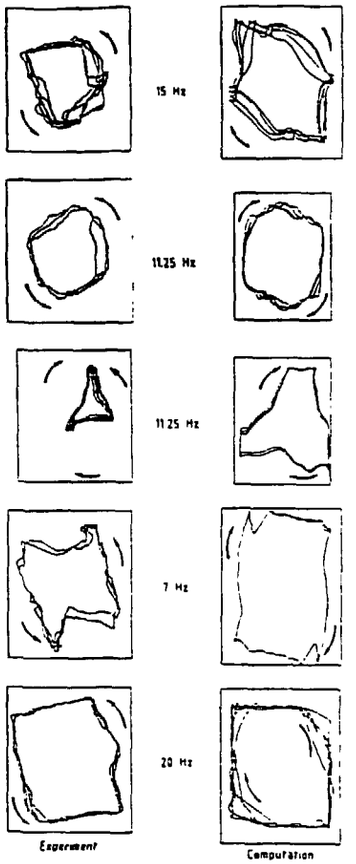

Fig 10 - Centered orbital vibrations lissajous plot of tube displacement for various driving frequencies

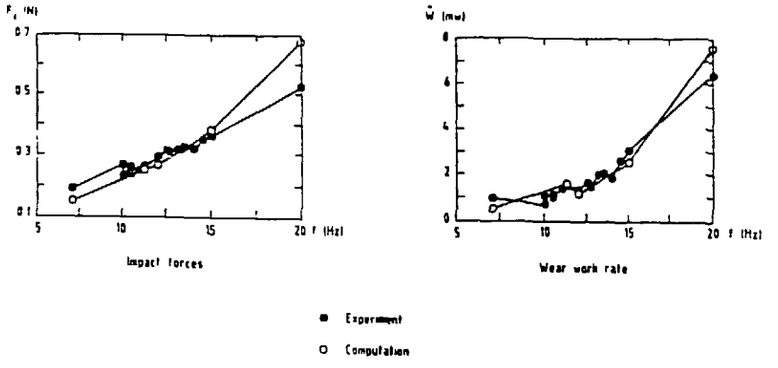

Fig 11 - Centered orbital vibrations at fixed excitation level Fx = Fy = 5N averaged impact forces and wear work rate versus excitation frequency

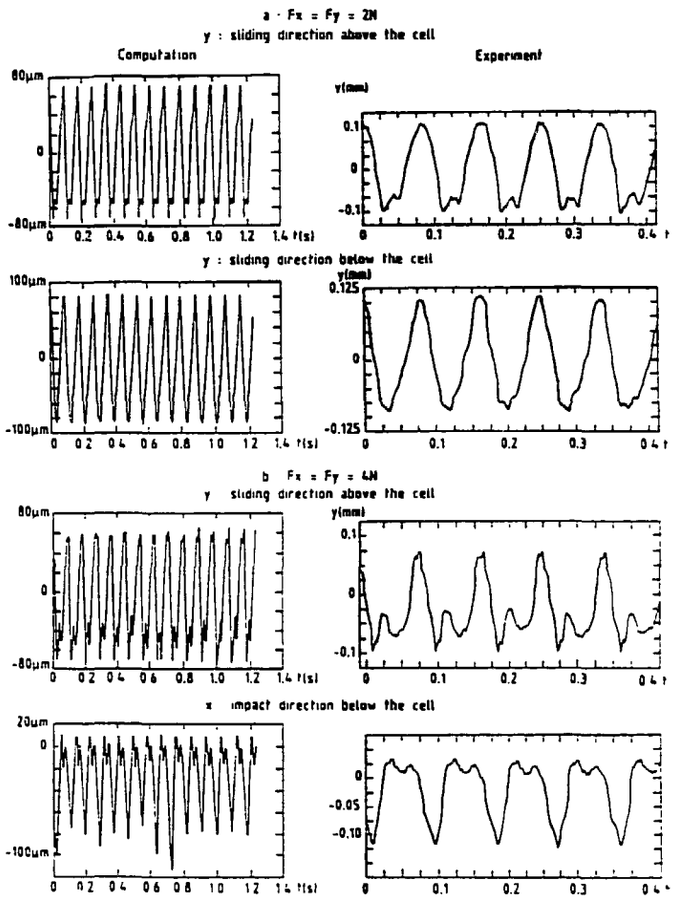

Fig 12 - Orbital vibration with a static preload 0 :N
on these plots time is in (s)

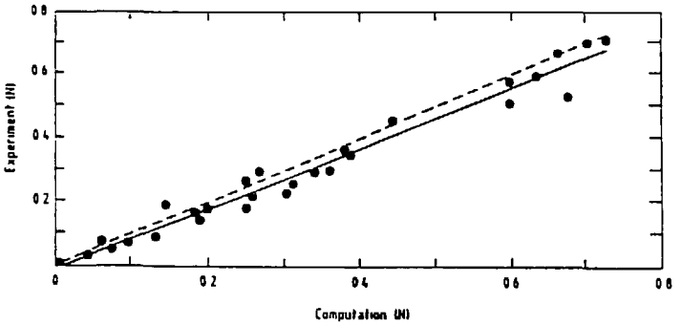

Fig 13 - Regression plot of averaged impact forces

solid line regression line

dashed line ideal line F_c computed = F_c measured

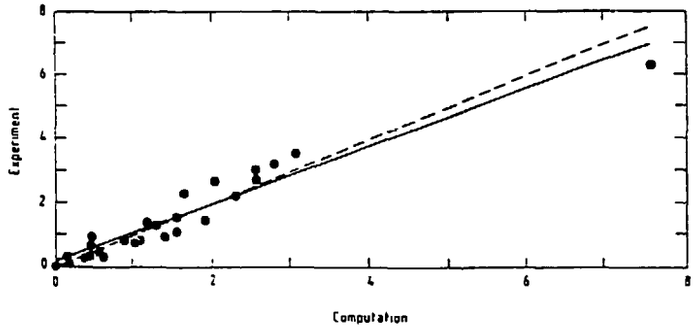

Fig. 14 - Regression plot of wear work rate in mW. Solid line is the regression line, and the dashed line is for the ideal line $\dot{W}$ computed = $\dot{W}$ measured